Simulation Study on Reseeding Link of an Air-Suc-tion Precision Tray Seeder

Hantao Zou , Mingge Wu * , Yunde Shen , Rui Xu , Chenghao Zhang , Minliang Wang

Posted Date: 30 June 2023

doi: 10.20944/preprints202306.2264.v1

Keywords: Air suction type; Precision seeder; Vibration; Seed grain distribution; Simulation analysis

Article

Simulation Study on Reseeding Link of an Air-Suction Precision Tray Seeder

Hantao Zou [1], Mingge Wu [1, 2, *], Yunde Shen [1, 2], Rui Xu [1], Chenghao Zhang [3] and Minliang Wang [1]

[1] School of Mechanical and Electrical Engineering, Wenzhou University, Zhejiang Province, China
[2] Institute of Laser and Optoelectronics Intelligent Manufacturing, Wenzhou University, Wenzhou, 325000, China
[3] Zhejiang Academy of Agricultural Sciences, Zhejiang Province, China
* Correspondence: wmg7810@wzu.edu.com; Tel.: +8613857783771

Abstract: Sowing accuracy is a critical factor in evaluating the precision of sowing equipment, and the sowing rate of the sowing equipment developed at home and abroad cannot reach 100 %, so this paper designs a seed reseeding device, aiming to improve the sowing rate secondly. Firstly, the structural composition of the seed reseeding device is introduced; secondly, according to the production object selected in this paper, kale seed (Jingfeng No.1), the best combination of factors and levels of the suction nozzle is 8 m/s inlet speed, 1.8 mm aperture, 18 mm lead and V-shaped nozzle by using orthogonal experiment; then, the EDEM software was used to conduct the vibration test, and it was found that the seed group "boils" steadily at about 15.13 mm (the depth of the reseeding tray is 23 mm), which can effectively improve the suction rate of the suction nozzle; finally, by combining the simulation results of the flow field using Fluent/ANSYS software and the spatial distribution of seeds, the number of seeds in the effective adsorption range of a single suction nozzle is about 4. The determined number of seeds, approximately 4, accounts for only 0.04% of the total number of seeds generated by the simulation. This percentage ensures high suction precision and a single seed rate, particularly under working conditions where a 72-hole tray is being sowed. In general, domestic sowing accuracy ranges from 90% to 95%. With this configuration, the purpose of improving the sowing rate twofold can be achieved.

Keywords: Air suction type; Precision seeder; Vibration; Seed grain distribution; Simulation analysis

1. Introduction

As a new seedling technology of modern agriculture, the sowing accuracy of seeding machine using this seedling technology is a key indicator of whether it can be promoted in the market and compete. Foreign technology is relatively mature automatic seeding line sowing accuracy of up to 95 % ~ 98 %, and equipped with an "empty hole detection" device. The current sowing accuracy of domestic tray seeders typically ranges from 90% to 95%, but in order to reduce the impact of missing cavities on seedling income, the conventional means is to arrange two to three workers to "check for leaks", which is not only increases the production cost, but also increases the labor intensity of workers [1-4]. Based on enhancing sowing accuracy and reducing production cost, this paper designs a seed reseeding device consisting of a needle seeder and an electromagnetic vibration mechanism.

The ST750 seeder from Williames, Australia, as shown in Figure 1, has a compact overall structure, high sowing accuracy, and high applicability, and can be widely used in vegetables, saplings, and garden plants, with a sowing pass rate of 96.7 % and a maximum sowing speed of 750 discs/h [5]. The YPSILON65 sowing equipment designed and produced by URBIONATI, Italy, is shown in Figure 2, with a sowing efficiency of up to 650 discs/h, equipped with a hole tray detection sensor at

Preprints (www.preprints.org) | NOT PEER-REVIEWED | Posted: 30 June 2023 doi:10.20944/preprints202306.2264.v1

the seed rower, with a scale at each link, able to be adjusted according to the size of the hole tray with a leakage rate of less than 2.3 % and a sowing rate of 97 % [6].

Figure 1. ST750 type planter

Figure 2. YPSILON65 type seeder

Qin Guangming et al. of Nanjing Institute of Agricultural Mechanization, Ministry of Agriculture, designed and developed the 2BSL-320 roller-type air-suction vegetable seeder as shown in Figure 3. On the basis of completing the automatic assembly line operation, an additional pulley set was installed to increase the maneuverability of the whole machine. The working efficiency could reach 600~800 discs/h, and the single seed rate ranged from 90.1 % to 98.5 %, the reseeding rate ranged from 1 % to 2.5 %, and the empty hole rate ranged from 0.9 % to 1.8 %, depending on the experimental object [7].

Figure 3. 2BSL-320 roller-type air suction type vegetable planter.

As a key component of precision seeding, the air-suction seed-metering device has the advantages of strong adaptability to seed size, low seed injury rate, high versatility, and adaptability, and has been vigorously developed and widely used in the R&D and design of seeding equipment at home and abroad [8-9]. By starting with the fundamental principle of the air-suction seeder and considering the advantages of the needle-type seed-metering device, this study employed the orthogonal experimental method to investigate and analyze the factors influencing the seed suction performance of the suction nozzle [10-12], and the best combination of factors level of the suction nozzle to satisfy the production object selected in this paper, kale seed (Jingfeng No. 1); ANSYS/ Fluent software was used to simulate the flow field to verify the mathematical model of seeds in "suspension" and to obtain the effective seed suction range of the suction nozzle.

In order to reduce the internal friction factor and increase the mobility of the bulk seeds, the widely used method is to make the seeds in the tray "boiling" state by vibrating the tray, which reduces the friction between the seeds and aids the suction device to suck the seeds to improve the suction accuracy [13-14]. The electromagnetic vibration mechanism designed in this paper uses the working principle of inputting high-frequency on-off current into the electromagnet to make the armature fixed on the elastic material, which is continuously attracted and reset to produce vibration. EDEM software is used for vibration simulation, in conjunction with the flow field simulation results

Preprints (www.preprints.org) | NOT PEER-REVIEWED | Posted: 30 June 2023 doi:10.20944/preprints202306.2264.v1

to map the effective seed absorption range of the seed reseeding link, and analyze the main factors affecting the seed absorption performance such as seed absorption efficiency and single grain rate according to the simulation results.

2. Mathematical model of reseeding link of air-suction precision tray seeder

A partial enlarged view of reseeding link of air-suction precision tray seeder is shown in Figure 4.

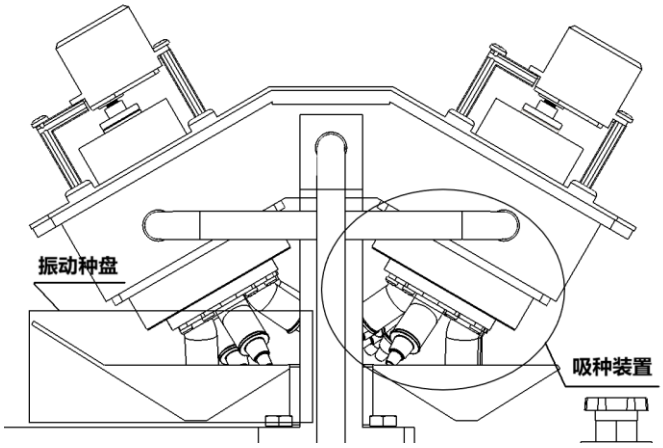

Figure 4. Partial enlarged view of reseeding link.

The seed reseeding link is mainly composed of seed suction device and vibration device, as shown in Figure 5 and Figure 6 respectively. The seed suction device is divided into a positive pressure zone and a negative pressure zone by the pressure plate, and the rotary motion of the rotary tray is controlled by the servo, so that the seed suction nozzle passes through the negative pressure zone and the positive pressure zone in turn to complete the seed suction and discharge; at the same time, the electromagnetic excitation device designed to increase the seed "mobility", strengthen the seed suction capacity and improve the single grain rate is fixed at the base of the seed tray. The base of the electromagnetic excitation device is fixed on both sides of the seed tray, and the electromagnetic relay is used to input current to the electromagnet, because the seed tray itself has a large mass, the vibration has less influence on it and does not interfere with the seed suction device [15-16].

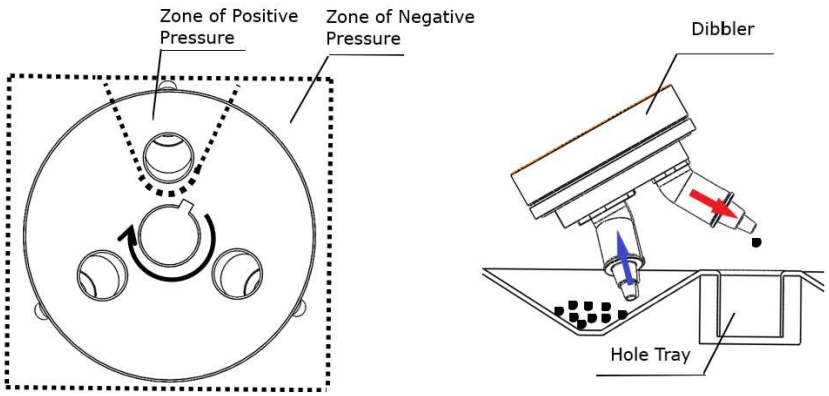

Figure 5. Principle diagram of seed suction device.

Preprints (www.preprints.org) | NOT PEER-REVIEWED | Posted: 30 June 2023 doi:10.20944/preprints202306.2264.v1

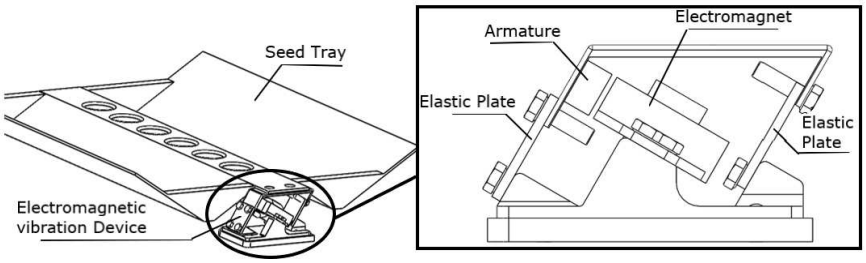

Figure 6. Structure diagram of electromagnetic excitation seed tray.

2.1. Mathematical model of seeds in a "suspended" state

The forces on the seeds in the "suspended" state are shown in Figure 7. The seeds in the "suspended" state are subjected to the fluid buoyancy force M, the fluid resistance to the seeds' bypassing F and the seeds' own gravity G. The magnitudes of these forces are [17]:

$$\mathrm{M} = \frac{m_s}{\rho_s}\rho_a g \tag{1}$$

$$F = \frac{1}{2}\rho_a C_d S_s {v_t}^2 \tag{2}$$

$$\mathrm{G} = m_s \mathrm{g} \tag{3}$$

Where: ρ_a -- fluid density, kg/m^3;

C_d -- resistance coefficient between seed and air, dimensionless;

S_s -- the projected area of seed in motion direction, m^2;

v_t -- relative velocity between seed and air, m/s;

ρ_s -- seed density, kg/m^3;

m_s -- seed weight, kg;

g -- the acceleration of gravity, m/s^2;

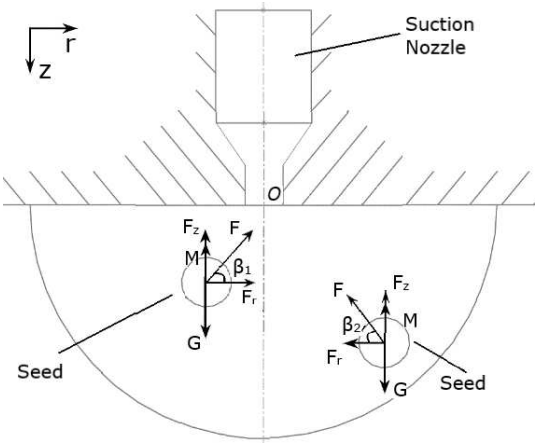

Figure 7. Seed stress analysis.

The stress equilibrium equation of seeds in a "suspended" state is:

$$F + M = G \tag{4}$$

$$F_Z + \frac{m_s}{\rho_s}\rho_a g = m_s g \tag{5}$$

At this time, the critical velocity of the seed is:

$$v_t = \sqrt{\frac{2cos\beta mg(\rho_s - \rho_a)}{C_d S_s \rho_s \rho_a}} \left(0 \le \beta < 90^\circ\right) \tag{6}$$

The precision tray seeder designed in this paper is mainly applicable to hole tray seeding of small grain-size seeds. Therefore, the more common small-grained seed, kale seed (Jingfeng No. 1)

Preprints (www.preprints.org) | NOT PEER-REVIEWED | Posted: 30 June 2023 doi:10.20944/preprints202306.2264.v1

[18], was selected as the object of study, and because of its approximate spherical shape, the drag coefficient at critical speed was obtained as:

$$C_d = \frac{4gd(\rho_s - \rho_a)}{3\rho_a {v_t}^2} \tag{7}$$

To determine the critical velocity of the seeds, the calculation using the table look-up method requires eliminating the v_t^2 term and using the factorless quantity $C_dR_e^2$.

$$R_e = \frac{v_t d\rho_a}{\eta} \tag{8}$$

Where: d -- seed diameter, mm;

η -- the dynamic viscosity of the fluid;

By substituting equation (7) into equation (6), we get:

$$C_d {R_e}^2 = \frac{4gd^3\rho_a(\rho_s - \rho_a)}{3\eta^2} \tag{9}$$

The equivalent diameter of kale seeds is 1.97 mm, the fluid density of air ρ_a is 1.23 kg/m^3, g is taken as 9.8 m/s^2, the dynamic viscosity of air η is 18.4×10^{-6} pa·s; the seed (mass) density of kale seeds ρ_s is 0.742×10^3 kg/m^2, which gives $C_dR_e^2$ as 2.7×10^5, and from the literature [19] the sphere of R_e and The maximum suspension speed v_t of single kale seeds is 3.7 m/s, which means that the kale seeds are in the range of needle suction nozzle, and the speed of "suspension" is 3.7 m/s.

2.2. Mathematical model of vibration mechanism

According to the structure of the seed tray, the electromagnetic vibration mechanism and the seed tray are considered as a whole and simplified to a mechanical model with parallel springs and dampers, and it is known from the working requirements and working principle that the seed tray only needs to carry out horizontal motion, and the simplified mechanical model established is shown in Figure 8 [20-21].

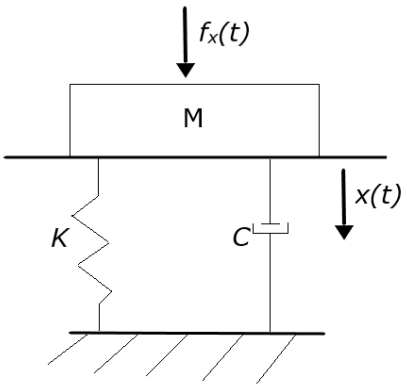

Figure 8. Simplified mechanical model for horizontal direction of the vibration system.

The vibration differential equation is:

$$M\ddot{x}(t) + C\dot{x}(t) + Kx(t) = f_x(t) \tag{10}$$

Where: M -- the mass of reseeding seed plate, kg;

K -- spring stiffness, N/m;

C -- viscous damping coefficient;

fx(t) -- horizontal excitation force on M, N;

x(t) -- displacement of M vibrating in the horizontal direction, m;

According to Equation (10), we can obtain:

$$\omega_x = \sqrt{\frac{K}{M}} \tag{11}$$

$$B = 2\xi\omega_x M \tag{12}$$

Where: ξ is the damping ratio of the system, with a general selection value ranging from 0.01 to 0.03.

Preprints (www.preprints.org) | NOT PEER-REVIEWED | Posted: 30 June 2023 doi:10.20944/preprints202306.2264.v1

According to equations (11) and (12), the natural frequency of horizontal vibration of the vibration system is only related to the mass of the tray and the stiffness of the vertical plate spring. Therefore, using SolidWorks software to conduct quality analysis on the three-dimensional model of the tray, the mass M=2.067 kg, plate spring parameters: Thickness h=2 mm, width b=20 mm, effective length of plate spring I=50 mm, elastic modulus E=2×10^5 N/mm^2, take the pressure coefficient η=1.05, the number of pieces i=1, the number of groups n=2, the theoretical stiffness of the spring can be calculated:

$$K = \frac{inEbh^3}{\eta I^3} = \frac{1 \times 2 \times 2 \times 10^5 \times 20 \times 2^3}{1.05 \times 50^3} \approx 487.6\ N/mm \tag{13}$$

Then the horizontal natural frequency of the vibration system:

$$\omega_x = \sqrt{\frac{K}{M}} = \sqrt{\frac{487.6}{2.067}} = 485\ rad/s \tag{14}$$

$$f_x = \frac{\omega_x}{2\pi} = \frac{485}{2\pi} \approx 77.2\ Hz \tag{15}$$

When the resonance value z=ω/ω_c (where ω is the excitation circle frequency and ω_c is the natural circle frequency of the system) meets z < 1, it is determined that the system has good working stability under this working condition.

If the excitation frequency f=50 Hz, then the excitation circular frequency ω=2πf=314 rad/s;

Then the horizontal resonance value is:

$$Z_x = \frac{\omega}{\omega_x} = \frac{314}{485} \approx 0.65 < 1 \tag{16}$$

Meet the resonant value requirements.

3. Simulation experiments and results analysis of the reseeding device

The main research of the seed suction device is to study the importance of the physical factors of the needle seeder affecting the performance of seed suction, and to design a needle seed suction nozzle suitable for the production object selected in this paper -- kale seed (Jingfeng No.1); at the same time, the process of seed suction will have the situation that there are multiple seeds in the range of the suction nozzle, the seeds collide with each other, the suction nozzle is clogged, and the adsorption of At the same time, there are multiple seeds in the nozzle area, seeds colliding with each other, clogging of the nozzle, and adsorption of multiple seeds, which will reduce the accuracy and single seed rate. Therefore, ANSYS/Fluent software was used to simulate the flow field and determine the effective adsorption range of the nozzle.

3.1. Orthogonal experiment and analysis of seed suction device

The needle-type seed suction nozzle serves as the crucial working component of the seed suction device. Its performance in seed suction is influenced by several key factors, including the inlet speed, aperture, lead, and mouth shape. According to the principle of an orthogonal test, the orthogonal table $L_9(3^4)$ with 3 levels and 4 factors was adopted.

The horizontal value of inlet velocity is selected according to the cross-section velocity range at the air supply source. The horizontal values of the aperture and lead are determined according to the parameter range of the target object. The mouth shape was modeled with SolidWorks software, and the model was changed according to different horizontal combinations of various factors. Then, the model was transferred to ANSYS/Fluent software for simulation analysis, and the optimal combination of various factor levels was finally determined. The three common types of needle seed suction nozzles are shown in Figure 9.

Preprints (www.preprints.org) | NOT PEER-REVIEWED | Posted: 30 June 2023 doi:10.20944/preprints202306.2264.v1

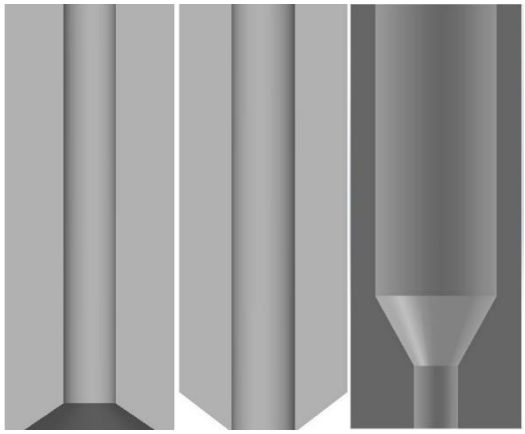

Table 9. Section view of the three-dimensional structure of suction nozzle.

Test factor setting and level coding, test scheme design, and simulation calculation results are shown in Tables 1 and 2.

Table 1. Test factors and level coding.

Level	Factor			
	A Inlet Velocity (m/s)	B Aperture (mm)	C Lead (mm)	D Mouth Shape
1	6	1.6	18	Type U
2	8	1.8	20	Type A
3	10	2.0	22	Type V

Table 2. Test scheme design and simulation results.

Level	Factor				The average flow rate of seed suction mouth(m/s)
	A Inlet Velocity (m/s)	B Aperture (mm)	C Lead (mm)	D Mouth Shape	
1	6	1.6	18	U	3.17
2	6	1.8	20	A	2.94
3	6	2.0	22	V	9.88
4	8	1.6	20	V	16.61
5	8	1.8	22	U	4.17
6	8	2.0	18	A	3.84
7	10	1.6	22	A	4.97
8	10	1.8	18	V	20.95
9	10	2.0	20	U	5.06

Statistical analysis software SPSS was used to process and analyze the orthogonal experimental data. The statistical results of the range analysis are shown in Table 3.

Table 3. Range analysis results.

Indicators	A Inlet Velocity (m/s)	B Aperture (mm)	C Lead (mm)	D Mouth Shape
K1	15.99	24.75	27.96	11.75
K2	24.62	28.06	24.61	12.4
K3	30.98	18.78	19.02	47.44
Mean K1	5.33	8.25	27.96	3.92
Mean K2	8.21	9.35	24.61	4.13

Preprints (www.preprints.org) | NOT PEER-REVIEWED | Posted: 30 June 2023 doi:10.20944/preprints202306.2264.v1

Mean K3	10.33	6.26	19.02	15.81
Range R	5	3.09	2.98	11.9
Optimal solution	10	1.8	18	3

In the orthogonal design experiment, if there is no repeated experiment and no blank term, the smallest sum of the square of the mean difference of one of the factors is often taken as the error estimation. It can be seen from Table 3 that the range value of the lead is the smallest, that is, the lead has the smallest influence on the results of the whole orthogonal experiment, so it is used as the error estimation to test the significance of the effects of other factors [22]. Factor C of the variable was eliminated, and SPSS software was used again for calculation. The results of the variance analysis were shown in Table 4.

Table 4. Results of variance analysis.

Source	Sum of Squares	*df*	Mean Square	*F*	*Sig.*
Model of Correction	330.482a	6	55.080	8.100	.114
Intercept	569.459	1	569.459	83.748	.012
An Inlet Velocity	37.736	2	18.868	2.775	.265
B Aperture	14.746	2	7.373	1.084	.480
D Mouth Shape	278.000	2	139.000	20.442	.047
C (Lead)	.279	2	.279		
Error	.279	2	.279		
Aggregate	900.22	9			
Total of correction	344.082	8			

* a.R squared =.960 (adjusted R squared =.842).

According to the results of range and variance analysis,

(1) The order of importance of each factor to the results of this orthogonal experiment is D mouth shape > A inlet velocity > B aperture > C lead; The order of the influence of each factor level on the experimental structure was as follows: $A_3 > A_2 > A_1$, $B_2 > B_1 > B_3$, $C_1 > C_2 > C_3$, $D_3 > D_2 > D_1$; The optimal factor horizontal combination is $A_3B_2C_1D_3$ (inlet velocity 8 m/s, aperture 1.8 mm, lead 18 mm, V-shaped nozzle);

(2) The D-shaped suction mouth had a significant effect on the experimental results (PD=0.047 < 0.05), and the V-shaped suction nozzle could obtain the maximum flow rate under the same conditions, and the best suction effect;

(3) The inlet velocity and aperture are the most important factors affecting the seed suction performance, and the lead only plays a role in stabilizing the flow field at the seed suction nozzle.

3.2. Simulation analysis of the flow field of the seed suction nozzle

The seed reseeding process will have the situation that multiple seeds can be adsorbed in the adsorption range of the suction nozzle, and the seeds collide with each other, and the problems of clogging of the suction nozzle and adsorption of multiple seeds will all reduce the accuracy and single seed rate of the reseeding process, and at the same time, it will cause unnecessary seed loss, which will further increase the production cost. The spatial distribution of the seed population is simplified to the case of spatial distribution of two seeds in the same axial profile horizontal plane, under the same radial height, and fluid simulation is performed.

Preprints (www.preprints.org) | NOT PEER-REVIEWED | Posted: 30 June 2023 doi:10.20944/preprints202306.2264.v1

Figure 10 and Figure 11 show the velocity of the flow field of the suction nozzle in the axial and radial profiles of the seed distribution, and the pressure distribution, respectively.

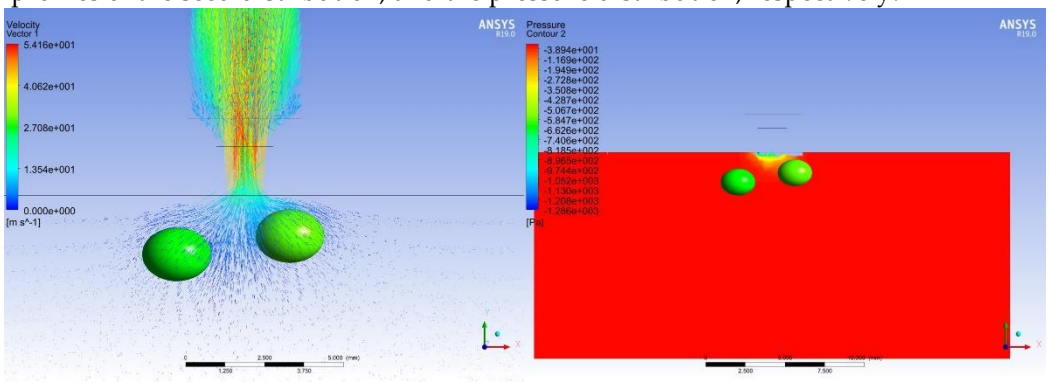

(a) Flow field velocity distribution of suction nozzle (b) Flow field pressure distribution of suction nozzle

Figure 10. Flow field distribution in an axial profile of seed suction nozzle.

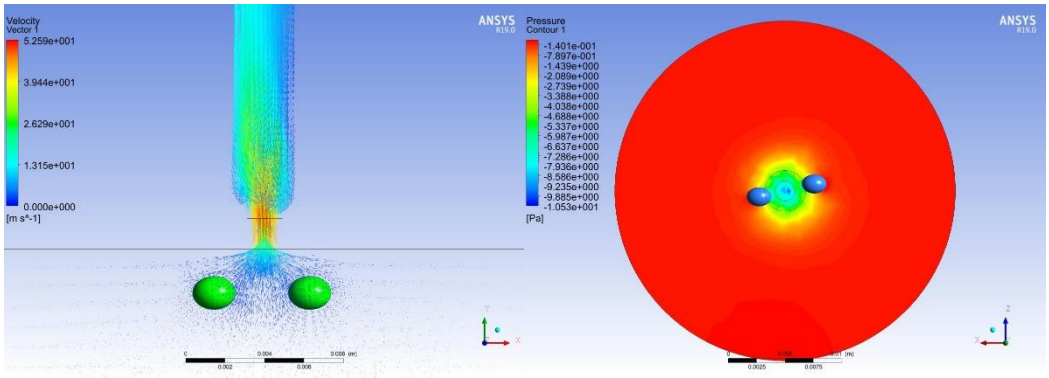

(a) Flow field velocity distribution of suction nozzle (b) Flow field pressure distribution of suction nozzle

Figure 11. Flow field distribution in radial profile of seed suction nozzle.

(1) From the axial profile flow field distribution diagram, it can be seen that near the suction nozzle, there is an obvious pressure gradient in the airflow field; the velocity vector lines drive the seeds and gather towards the suction nozzle, the closer the seeds are to the suction nozzle, the more dense the velocity vector lines around the perimeter, the greater the adsorption force on them, and they are more easily adsorbed, and the attachment velocity of the suction nozzle can reach 27.08 m/s, far exceeding the maximum suspension velocity of single kale seeds;

(2) Under the same radial profile, the velocity vector lines around the seed circumference and at the same height are distributed more consistently; from the pressure distribution cloud, it can be seen that the pressure has an obvious fan-shaped distribution, and the pressure value gradually increases from the outside to the inside, and the pressure value of the seed suction nozzle attachment corresponds to the velocity range, which meets the velocity requirement of seed adsorption;

(3) After comprehensive measurement, it is concluded that the maximum suspension velocity of single kale seeds is greater than 3.7m/s in the range of spheroid composed of -2.24 mm＜x＜2.23 mm, -5.87 mm＜y＜-1.66 mm and -2.76 mm＜z＜2.82 mm with the plane of the seed suction nozzle as the reference plane, and the effective seed suction range of the seed suction nozzle is simplified to a hemisphere with a radius of about 2.23 mm hemisphere.

4. Simulation experiments and results analysis of the seed vibration device

By analyzing the displacement and force of the seeds in the “boiling” state and verifying the rationality of the mathematical model, we also simulated the seed reseeding process by combining the spatial distribution of the seed population in the “boiling” state and the installation position of

Preprints (www.preprints.org) | NOT PEER-REVIEWED | Posted: 30 June 2023 doi:10.20944/preprints202306.2264.v1

the needle seeder, and analyzed the main factors affecting the seed absorption performance, such as seed absorption efficiency and single seed rate [23-24].

4.1. model setup and simulation pre-processing

(1) The 3D model of the vibrating seed tray was imported into EDEM software, and the bottom surface of the seed tray was set as the reference surface (the depth of the seed tray is 23 mm);

(2) The kale seeds (Jingfeng No. 1) are similar to spheres, and there is no adhesion force on the seed surface, so the Hertz-Mindlin no-slip contact model is selected. According to the length, width, and height of kale seeds, that is, the triaxial dimension is 2.19 mm×1.79 mm×1.62 mm, the parameters of mechanical and physical properties of seeds are: Poisson's ratio 0.49, shear modulus 3.97×10^{8} pa, density 742 kg/m^{3}, inter-seed recovery coefficient 0.6, static friction coefficient 0.5, dynamic friction coefficient 0.01, discrete elements are established in EDEM software model, as shown in Figure 12;

(3) Set the vibration frequency as 77.2 Hz, amplitude 1.2 mm, total simulation time as 6 s, and save the data every 0.1 s.

(4) Establish the seed factory and set its location and shape to produce kale seeds in the quantity of 10000. The kale granule body in the vibrating seed tray was arbitrarily selected for marking and recorded as numbers 7, and 84, and the kale seed granule body with number 84 is shown in Figure 13.

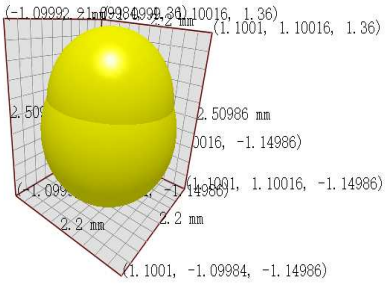

Figure 12. EDEM model of kale seed

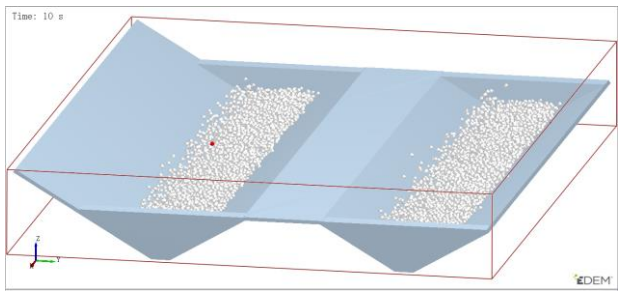

Figure 13. Simulation diagram of vibration process

4.2. Analysis of simulation results

Figure 14 (a), (b), (c) shows the curves of kale seeds and seed population displacement with time for numbers 84, and 7, respectively.

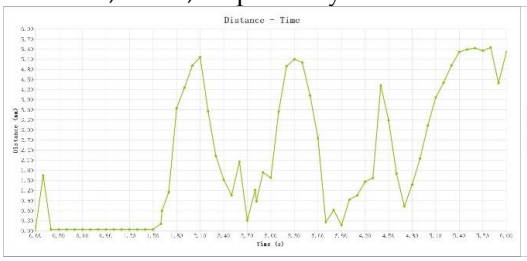

(a) No. 84

(b) No. 7

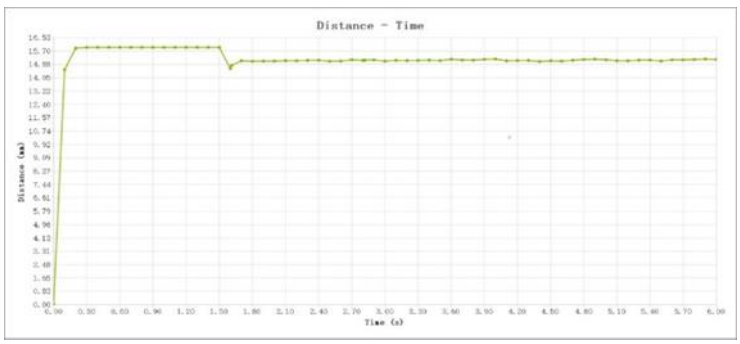

Preprints (www.preprints.org) | NOT PEER-REVIEWED | Posted: 30 June 2023 doi:10.20944/preprints202306.2264.v1

(c) Group of seeds

Figure 14. Graph of displacement and time of seed population.

Figure 15 (a), (b), and (c) shows the curves of kale seeds and seed population force with time for numbers 84, and 7, respectively.

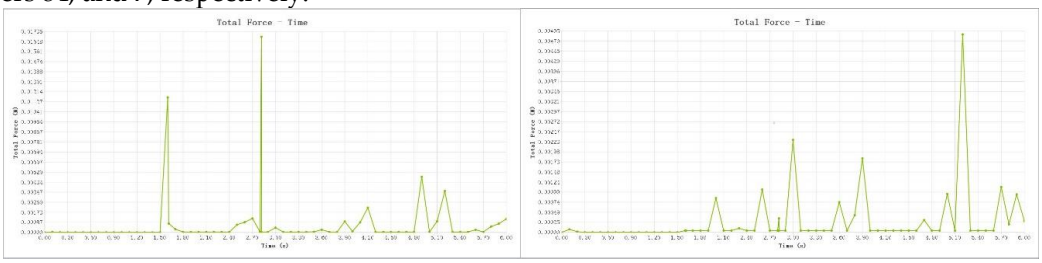

(a) No. 84 (b) No. 7

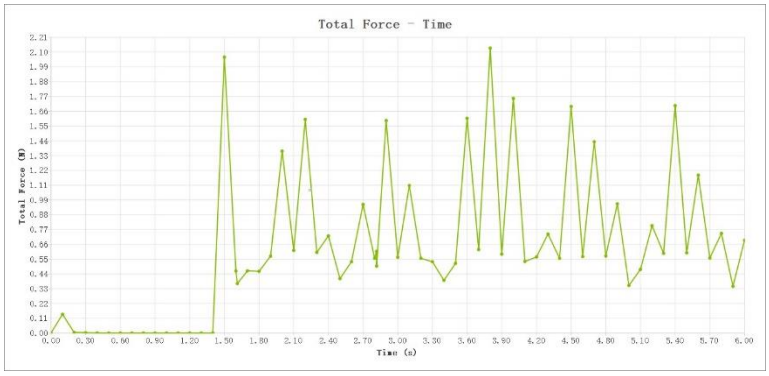

(c) Group of seeds

Figure 15. Graph of force and time of seed population.

(1) 0~1.5 s for the seed plant to generate seeds and place them on the seed tray statically; 1.5 s later, the vibration starts. From Figure 14, it can be seen that the displacement peak of No. 84 reaches about 5.10 mm, the displacement peak of No. 7 reaches about 5.67 mm, and the displacement curve of seed group shows a trend of rising and then falling until relatively stable movement, and finally stabilizes at about 15.13 mm. It shows that the "boiling" height is suitable under the theoretical calculated amplitude value, and the seed group in the "boiling" state is basically inside the seed tray, and only very few seeds pop out of the seed tray, which meets the working requirements of the vibration device.

(2) From Figure 15(a) (b), it can be seen that the force curve of the single seed is irregular under the change of time, mainly because of the interaction force between the particles within the population, the tangential friction force of the seed tray on the seeds, the inertia force and the gravity of the seeds themselves are more complex under the joint action of multiple forces with time; Figure (c) after the vibration starts, the force curve of the seed population is similar to the simple harmonic vibration curve, which means that the whole population is in a good "boiling" height. This indicates that the whole population is in a good "boiling" state, which helps to absorb seeds.

4.3. Simulation analysis of the spatial distribution of seeds during reseeding

The physical analysis of the seed reseeding tray was carried out by Solidworks software, and the effective working length was measured to be 240 mm. Combined with the effective seed suction range of the seed suction nozzle in Section 3, the total working space of the seed suction device was calculated to be a rectangular body of 240 mm in length, 4.46 mm in width, and 2.23 mm in depth.

The results of the vibration simulation test showed that the seed cluster kept a relatively stable "boiling" state at 15.13 mm from the reference surface (bottom of the seed reseeding tray) after the

Preprints (www.preprints.org) | NOT PEER-REVIEWED | Posted: 30 June 2023 doi:10.20944/preprints202306.2264.v1

vibration started. The structure of the seed reseeding link is designed to avoid the interference problem when the seed suction device works, and each two seed suction devices are 82mm apart, and the horizontal cross-section of the stable "boiling" state of the seed cluster and the installation position of the seed suction device are combined to establish the equivalent diagram of the reseeding process of the seed reseeding tray (single column) as shown in Figure 16.

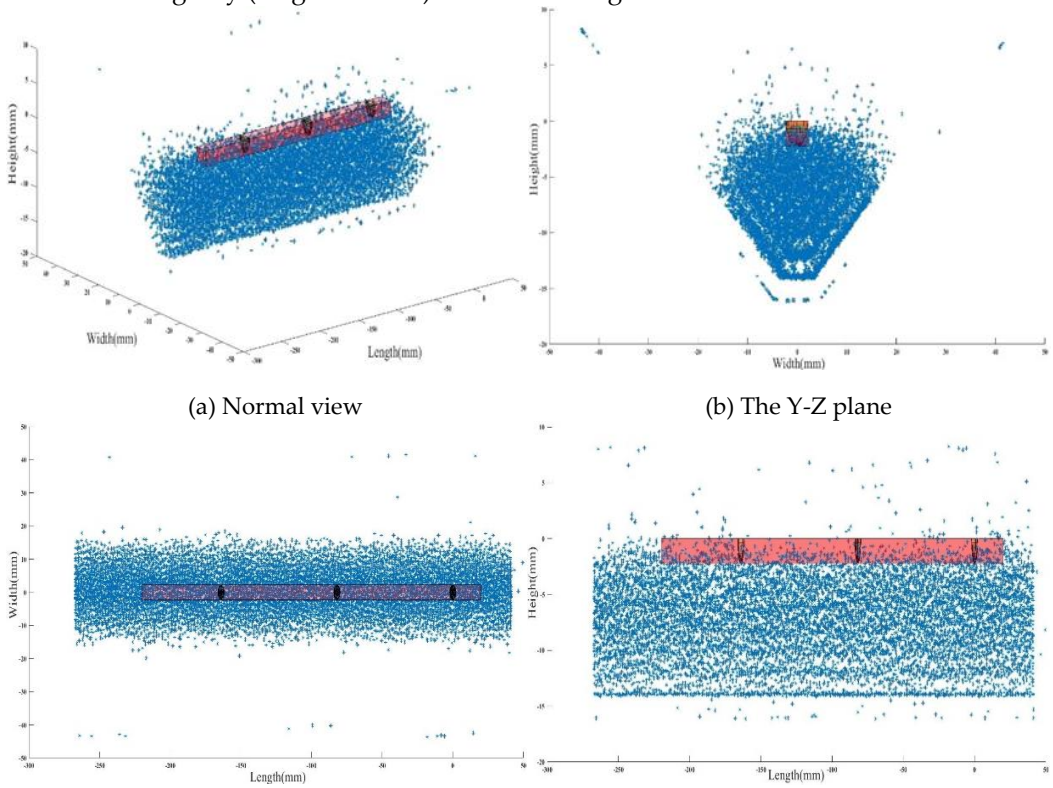

(a) Normal view (b) The Y-Z plane

(c) The X-Y plane (d) The X-Z plane

Figure 16. Reseeding process diagram of reseeding seed tray (single row).

The spatial distribution of the seed population from 5.9 to 6 s in the vibration simulation was selected for this experiment.

The actual number of seeds produced by the seed factory in the vibration simulation is 9291 (single row), and it can be seen from the normal view that only a very small number of seed positions are outside the normal working range of the vibrating seed tray, which can be neglected; it can be seen from the three plane views that the stratification of the seed population in the "boiling" state is more obvious, and the vibration range is more stable. In particular, it can be seen that the seed interval increases significantly from the bottom to the top, and the seed group distribution in the horizontal section of the "boiling" state is the most ideal.

Combined with the data, the seeds in the total working space of the nozzle accounted for 4.05 % of the total number of seeds, i.e. 376 seeds, and the effective adsorption range of a single nozzle accounted for 0.98 % of the total working space of the nozzle, i.e. the number of seeds in the effective adsorption range of a single nozzle was about 4 seeds.

In domestic sowing accuracy is generally 90 % ~ 95 %, sowing a 72-hole hole tray, a single servo-driven needle suction nozzle only needs to work 1.5 times, therefore, in the actual production operation, the appropriate reduction of the total number of seeds in the reseeding seed tray, can ensure the suction accuracy, single seed rate at the same time, to avoid the possibility of seed collision, to achieve the effect of secondary improvement of sowing accuracy.

5. Conclusions

 doi:10.20944/preprints202306.2264.v1

By considering practical production requirements and utilizing a combination of theoretical calculations and simulation tests, the precision tray seeder studied in this paper has led to the following conclusions:

(1) The structural composition of the seed reseeding device of the hole tray precision seeder is described, and the maximum seed suspension speed of 3.7 m/s and the vibration frequency of 77.2 Hz is calculated based on the production object, kale seed (Jingfeng No.1), and the physical parameters related to the reseeding seed tray.

(2) By orthogonal test method, it is concluded that the order of importance of each factor of seed suction nozzle on seed suction performance is nozzle type > inlet speed > aperture diameter > guide stroke, and the best combination of factors is inlet speed 8 m/s, aperture diameter 1.8 mm, guide stroke 18 mm, and V-type nozzle. Among them, V-shaped nozzle can obtain the maximum flow rate under the same conditions and has the strongest seed suction capacity. The inlet velocity and the size of the aperture are the main influencing factors of the seed suction performance, and the guide stroke has a weak influence on the seed suction performance and only plays the role of stabilizing the flow field.

(3) EDEM software was used to establish a discrete model of kale seeds, and the vibration process was simulated and analyzed. The test results showed that the displacement curve of the seed group was in a stable "boiling" state during the vibration process, the force curve of the seed group was similar to the simple harmonic vibration curve, and the vibration effect was good, which was helpful for the reseeding process.

(4) Combining the flow field simulation results with the spatial distribution of seeds, the total working space of the seed suction device is obtained, and the percentage of seeds in the effective suction range of the suction nozzle is 4.05 %, i.e. 376 seeds, and the effective suction range of a single suction nozzle accounts for 0.98 % of the total working space of the suction nozzle, i.e. the number of seeds in the effective suction range of a single suction nozzle is about 4, which ensures the precision of suction and the single seed rate of the seed reseeding process. This ensures the precision of seed suction and single seed rate in the seed reseeding link, and can improve the precision of sowing twice.

6. Acknowledgments

This study was supported by Key R&D Project in Zhejiang Province No. 2019C02019 and Wenzhou Municipal Key Science and Research Program (ZN2022001). The School of Mechanical and Electrical Engineering of Wenzhou University also provided technical support. The author also thanks the students who helped me during the research: Rui Xu, Mingshao Chen, Jiachen Huang, Weihao Ni, and Tao Qin.

References

1. Karayel, D.; Barut, Z B.; zmerzi, A. Mathematical modelling of vacuum pressure on a precision seeder. *Biosyst Eng* **2004,** 87(4), 437-444.
2. Arzu, Y.; Adnan, D. Optimisation of the seed spacing uniformity performance of a vacuum-type precision seeder using response surface methodology. *Biosyst Eng* **2007,** 97(3), 347-356.
3. Gaikwad, B B.; Sirohi, N P S. Design of a low-cost pneumatic seeder for nursery plug trays. *Biosyst Eng* **2008,** 99(3), 322-329.
4. Singh, R C.; Singh, G.; Saraswat, D C. Optimization of design and operational parameters of a pneumatic seed metering device for planting cottonseeds. *Biosyst Eng* **2005,** 92(4), 429-438.
5. Zheng, G.; Liu, J.; Nie X.B.; Li, B.M.; Wang, C.D. Application of plant seedling technology and equipment for plant vegetable. *Agricultural Engineering Technology* **2019,** 39(10), 60-65.
6. Yang, Q.Z.; Xu, L.; Shi X.Y.; Ahamd, Ibrar.; Mao, H.P.; Hu, J.P.; Han, L.H. Design of seedlings separation device with reciprocating movement seedling cups and its controlling system of the full-automatic plug seedling transplanter. *Comput Electron Agr* **2018,** 147, 131-145.
7. Qin, G.M.; Zhao, Y.; Xiao H.R.; Jin, Y.; Wu, Y.D.; Li, Q. Development and performance test of 2BSL-320 drum suction type vegetable precision sowing machine. *Journal of Chinese Agricultural Mechanization* **2015,** 36(6), 68-71.

8. Yu, J.J.; Liao, Y.T.; C, S.; Yang, S.; Liao, Q.X. Simulation analysis and match experiment on negative and positive pressures of pneumatic precision metering device for rapeseed. *Int J Agr Biol Eng* **2014,** 7(3), 1-12.
9. Arzu, Y.; Adnan, D. Measurement of seed spacing uniformity performance of a precision metering unit as function of the number of holes on vacuum plate. *Measurement* **2014,** 10(56), 128-135.
10. Liu, H.T. Study on Mechanical-Electron-Magnetismco-Simulation of Electromagnetic Vibrated Seed-Metering Device. Master's thesis, Guangxi University, Guangxi, China, 2013.
11. Luo, X.; Hu B.; Dong, C.W. Simulation experimental study on the adsorption properties of suction nozzle of the air-suction precision tray seeder. *Journal of Hebei Agricultural University* **2011,** 34(01), 111-113+118.
12. Chen, J.; Li, Y.M.; Wang, X.Q.; Zhao, Z. Finite Element Analysis for the Sucking Nozzle Air Field of Air-suction Seeder. *Transactions of the Chinese Society for Agricultural Machinery* **2007,** 09, 59-62.
13. Chen, J.; Zhou, H.; Zhao, Z.; Li, Y.M.; Gong, Z.Q. Analysis of Rice Seeds Motion on Vibrating Plate Using EDEM. *Transactions of the Chinese Society for Agricultural Machinery* **2011,** 42(10), 79-83+100.
14. Yazgi, A.; Degirmencioglu, A. Optimisationof the seed spacing seeder using response surface methodology. *Biosyst Eng* **2007,** 97(3), 347-356.
15. Zhao, Z.; Li, Y.M.; Chen, J.; Xu, L.Z. Influence of seeds spatial distribution on suction performance of precision vacuum seeder. *Journal of Jiangsu University (Natural Science Edition)* **2009,** 30(06), 559-563.
16. Zhao, Z.; Li, Y.M.; Liang, Z.W.; Gong, Z.Q. DEM simulation and physical testing of rice seed impact against a grain loss sensor. *Biosyst Eng* **2013,** 116(4), 410-419.
17. Zhang, Z.L.; Wang, J.L.; Cheng, H.Q.; Zhang W.Z.; Airflow Simulation and Optimization Design for Vegetable Pneumatic Seed Supply Device-Based on ANSYS/FOTRAN. *Journal of Agricultural Mechanization Research* **2011,** 33(04), 43-45.
18. Li, Q.C. Mechanism Analysis and Experimental Study on Scoop Type Precision Seed Metering Device for Small Size Vegetable Seeds. Master's thesis, Northeast Agricultural University, Heilongjiang, China, 2020.
19. Zhou, Z.E. *Physical Properties of Bio-Materials.* Beijing: agriculture press, Beijing, China, 1994; pp. 1-100.
20. Chen, J.; Zhou, H.; Zhao, Z.; Li, Y.M.; Gong, Z.Q. Analysis of Rice Seeds Motion on Vibrating Plate Using EDEM. *Transactions of the Chinese Society for Agricultural Machinery* **2011,** 42(10), 79-83+100.
21. Tang, J.; Yan, H.R.; Yang, H. Design and Simulation of a Novel Electromagnetic Vibration Feeder. *Journal of Xihua University(Natural Science Edition)* **2009,** 28(02), 12-16+24.
22. Yang, W.W. Research on Cylinder Precision tomato Seeder Based On The Pneumatic Suspension Seed Supply. Master's thesis, Shihezi University, Xinjiang, China, 2014.
23. Zhang, S.P.; Chen, J.; Li, Y.M. Analysis of seeds "Boiling" motion on vibrational air-suction tray seeder. *Transactions of the Chinese Society of Agricultural Engineering* **2008,** 07, 20-24.
24. Gong, Z.Q.; Chen, J.; Li, Y.M. Seed Force in Airflow Field of Vacuum Tray Precision Seeder Device during Suction Process of Seeds. *Transactions of the Chinese Society for Agricultural Machinery* **2014,** 45(06), 92-97+117.